doi.org/10.36721/PJPS.2026.39.12.346.1

Therapeutic efficacy of naloxone hydrochloride combined with hemoperfusion in toxic acute renal failure via the oxidative stress/Nrf2 pathway

Yin Zhu[1], Huichun Sun[2], Qiuyang Wang[3], Yong Sheng[1], Yanli Li[4] and Qiang Zhang[2*]

[1]Department of Hematology and Nephrology, The First Affiliated Hospital of Qiqihar Medical University, Qiqihar, Heilongjiang, 161000, China

[2]Department of Emergency Medicine, The First Affiliated Hospital of Qiqihar Medical University, Qiqihar, Heilongjiang, 161000, China

[3]Department of Cardiovascular Medicine, The First Affiliated Hospital of Qiqihar Medical University, Qiqihar, Heilongjiang, 161000, China

[4]Department of Hemodialysis, The First Affiliated Hospital of Qiqihar Medical University, Qiqihar, Heilongjiang, 161000, China

Abstract: **Background**: Toxic acute renal failure (ARF) involves severe oxidative stress. The Nrf2 pathway is a key antioxidant defense mechanism. **Objectives**: To investigate whether naloxone combined with hemoperfusion alleviates oxidative injury via Nrf2 activation in toxic ARF. **Methods**: In this single-center retrospective cohort study at Qiqihar Medical University Hospital, 67 patients were enrolled through medical record screening. The control group (n=39) received hemoperfusion alone; the observation group (n=28) received additional intravenous naloxone (0.8 mg bolus + 2.0 mg/24 h infusion for 7 days). Renal function and oxidative markers were assessed before treatment, at 24 h and day 7. Multivariate regression analysis was used to adjust for confounding factors. Separately, 30 rats were randomized into control, model and treatment groups (n=10 each). The treatment group received intraperitoneal naloxone (1.0 mg/kg) plus simulated hemoperfusion. **Results**: After adjusting for baseline imbalances, combined therapy was independently associated with significant reductions in Scr and BUN in patients (adjusted $\beta = -8.52$, 95% CI: -12.37 to -4.67, $P < 0.001$) and with significant improvements in renal function and histopathology in rats. Combined therapy decreased tubular injury markers (β2-MG, KIM-1, NGAL, L-FABP) in rats. Mechanistically, it was associated with activation of the Nrf2/HO-1/NQO1 pathway, enhanced SOD activity and reduced MDA levels. Improvements were time-dependent (24 h to day 7). **Conclusions**: Naloxone combined with hemoperfusion activates the Nrf2 pathway, attenuates oxidative stress and improves renal function in toxic acute renal failure.

Keywords: Hemoperfusion; Naloxone; Nrf2; Oxidative stress; Toxic acute renal failure

Submitted on 13-10-2025 – Revised on 08-04-2026 – Accepted on 22-04-2026 – Available online on 28-08-2026 – Published on 01-12-2026

INTRODUCTION

Toxic acute renal failure (ARF) is a common critical condition in clinical practice, characterized by sudden onset and rapid progression (Yu *et al*., 2024). Currently, hemoperfusion is widely used as an effective extracorporeal method to remove toxins in the treatment of poisoning-related disorders (Zou *et al*., 2026). Hemoperfusion alleviates the renal burden and creates conditions for renal function recovery by adsorbing and clearing exogenous toxins, inflammatory mediators and cytokines from the circulation. However, recent studies indicate that patients with renal injury often experience multi-system internal environmental disturbances and a single hemoperfusion technique cannot completely remove all toxic metabolites from the blood. Therefore, relying solely on hemoperfusion often makes it difficult to fully reverse established tubular injury (Yang *et al*., 2025). Consequently, identifying drugs that can synergize with hemoperfusion to intervene in the pathophysiological mechanisms of renal injury has become a current research hotspot.

**Corresponding author:* e-mail: xingyou6140164@126.com

Nuclear factor erythroid 2-related factor 2 (Nrf2) not only regulates cellular redox homeostasis but also partially suppresses inflammatory responses (Alam *et al*., 2023; Sun *et al*., 2023). Normally, Nrf2 binds to Keap1, which is then recognized and degraded by the ubiquitin-proteasome system. When cells are exposed to oxidative stress or electrophilic agents, Nrf2 dissociates, rapidly translocates into the nucleus and binds to antioxidant response elements (AREs). This process subsequently activates transcription of downstream genes, such as heme oxygenase-1 (HO-1) and NQO1, thereby enhancing cellular antioxidant capacity (Kurzhagen *et al*., 2023). Experimental evidence demonstrates that activation of the Nrf2 pathway confers significant renoprotection in kidney injury models. Nrf2 agonists markedly improve renal function and reduce histopathological changes, whereas inhibition of the pathway worsens renal damage (Lin *et al*., 2023).

Naloxone hydrochloride, a classical opioid receptor antagonist, has long been primarily used to reverse central respiratory depression caused by opioid overdose (Ibrahim *et al*., 2023; Taghavi *et al*., 2023). However, recent studies have revealed that naloxone possesses biological activities beyond its classical pharmacological effects. Research

shows that naloxone can reduce the release of pro-inflammatory cytokines through non-opioid receptor pathways; simultaneously, it can inhibit microglial activation, thereby reducing reactive oxygen species formation and exerting antioxidant and anti-apoptotic effects (Ibrahim *et al*., 2023). To date, studies on naloxone combined with hemoperfusion for treating toxic acute renal failure are rarely reported and its regulatory effect on the Nrf2 pathway and its molecular mechanisms remain unclear.

This study, based on the oxidative stress/Nrf2 signaling pathway, aimed to explore the therapeutic efficacy and underlying mechanisms of naloxone hydrochloride combined with hemoperfusion in toxic acute renal failure. Through a combination of clinical observations and animal experiments, the study systematically evaluated the impact of this combined therapy on renal function markers, histopathological injury and expression of key molecules in the Nrf2 pathway. The objective is to provide new therapeutic strategies and theoretical support for clinical management.

MATERIALS AND METHODS

Reagents and instruments

Naloxone hydrochloride (Wuhan Jingkangen Biopharmaceutical Co., Ltd.); cisplatin (Kerei Biotechnology Co., Ltd.); ether (Yangzhou Sanhe Chemical Co., Ltd.); ultra-low temperature freezer at –80 °C (Shanghai Daluo Scientific Instruments Co., Ltd., DW-86L158); paraffin, ethanol, xylene (Shanghai Sengkailong Chemical Co., Ltd.); vacuum blood collection tubes (Cangzhou Fukang Medical Ltd.); low-speed centrifuge (Shanghai Anting Scientific Instruments, KA-1000); human ELISA kits (Shanghai Future Industrial Co., Ltd.); sterile EP tubes (Tianjin Jiankang Technology Co., Ltd.); ELISA kits (Jiangsu Kejing Biotechnology Co., Ltd.); optical microscope (Pumai Precision Medical Technology Co., Ltd., CSIM100); 4% paraformaldehyde solution (Xinzhi Source Chemical Co., Ltd.); TRIzol reagent (Guangzhou Weijia Technology Co., Ltd.); staining kits (Shanghai Gefan Biotechnology Co., Ltd.); BCA protein assay kit (Shanghai Zhuoli Biotechnology Ltd.); reverse transcription kit (Yisheng Biotechnology Co., Ltd., Cat. No. 13894ES60); primer sequences (Hepeng Biotechnology Co., Ltd.); real-time PCR system (Guangzhou Jianlun Biotechnology Co., Ltd.); primary and secondary antibodies (Shanghai Jingkang Bioengineering Co., Ltd.).

Research methods

Selection and grouping of subjects

Clinical study: This was a single-center, retrospective cohort study. Patients who were diagnosed with toxic acute renal failure and met the indications for hemoperfusion at the First Affiliated Hospital of Qiqihar Medical University from January 2023 to June 2025 were enrolled as study subjects. Clinical data were retrospectively collected through the hospital's electronic medical record system.

Inclusion criteria: (1) Met the diagnostic criteria for toxic acute renal failure (Wang *et al*., 2024); (2) Received hemoperfusion treatment; (3) Complete clinical data, including the primary outcome indicators required for the study; (4) Age ≥ 18 years.

Exclusion criteria: (1)Combined with severe cardiac or hepatic dysfunction; (2)Allergic to naloxone hydrochloride; (3)Cognitive deficits, audiovisual impairments, or mental illness; (4)Abnormal coagulation function indicators or autoimmune disorders; (5) Recent (within 2 weeks) treatment with nephrotoxic drugs or corticosteroids; (6) Pregnancy or lactation.

Grouping: Based on whether naloxone hydrochloride was combined during the treatment period, enrolled patients were divided into two groups according to their actual treatment regimens. Control group: Received conventional hemoperfusion alone.Observation group: Received naloxone hydrochloride combined with conventional hemoperfusion (intravenous bolus of 0.8 mg, followed by continuous infusion of 2.0 mg/24 h for 7 days). The two groups of patients were naturally formed according to the actual clinical medication situation and were not randomly assigned. The process of participant screening, enrollment and grouping is illustrated in the flow diagram (Fig. S1).

Sample size calculation: Given the retrospective design of this study, a conventional a priori sample size estimation was not applicable *(*Abdul Rahman *et al., 2025)*. Based on the actual enrollment during the study period, a total of 67 patients (39 in the control group and 28 in the observation group) were enrolled according to the above inclusion and exclusion criteria through medical record screening. The unequal sample sizes between the two groups resulted from actual clinical treatment decisions and no artificial matching or sample size adjustment was performed. Post-hoc power analysis, using the observed between-group difference in serum creatinine reduction at day 7 (13.5 μmol/L) and a pooled standard deviation of 14.2 μmol/L at $\alpha = 0.05$ (two-sided), yielded a statistical power of 0.82, confirming that the sample size was adequate to detect a significant difference between the two groups.

Animal study: Thirty SPF-grade male Sprague-Dawley rats (6-8 weeks old, weighing 180- 220 g) were purchased from Speike (Beijing) Experimental Animal Technology Co., Ltd. (License No.: SCXK (Beijing) 2022-0012). They were housed in the Laboratory Animal Center of Qiqihar Medical University (License No.: SYXK (Heilongjiang) 2023-005) at a temperature of 22-25°C, humidity 50%-60%, with a 12-hour light/dark cycle, free access to food and water and acclimatized for one week before the

experiment. All animal experimental procedures followed the US National Institutes of Health's "Guide for the Care and Use of Laboratory Animals"(National Research Council, 2011). Rats were randomly divided into 3 groups using a random number table, with 10 rats per group: Control group: 10 male SD rats received an intraperitoneal injection of an equal volume of normal saline; Model group: 10 male SD rats received a single intraperitoneal injection of cisplatin (6 mg/kg) to establish a toxic acute renal failure model; Treatment group: 10 male SD rats received an intraperitoneal injection of naloxone hydrochloride (1.0 mg/kg) at 24 h post-modeling and received simulated hemoperfusion at 6 h post-modeling. A blinded design was used during the experiment, with personnel not involved in grouping and intervention completing index detection and statistical analyses.

Method of simulated hemoperfusion in rats: Rats in the treatment group underwent simulated hemoperfusion at 6 h post-modeling. Rats were anesthetized with isoflurane inhalation and fixed. The right common carotid artery and left external jugular vein were isolated and silicone catheters were inserted and connected to the perfusion device. The perfusion system consisted of a miniature peristaltic pump, a self-made miniature activated carbon perfusion device (containing 20 mg of coated activated carbon adsorbent) and a thermostat. The priming solution was normal saline containing heparin (50 U/mL). Before starting perfusion, heparin (100 U/kg) was administered via the carotid artery catheter for systemic anticoagulation. During perfusion, blood was drawn from the carotid artery, passed through the perfusion device via the peristaltic pump at a flow rate of 0.5 mL/min and then returned to the external jugular vein. The entire perfusion process lasted 2 hours, during which a thermostat maintained the blood temperature at approximately 37°C. After perfusion, the catheters were removed, blood vessels were ligated and the skin incision was sutured. Rats in the control and model groups underwent only vascular isolation and catheter insertion, without being connected to the perfusion device. All other procedures were the same as in the treatment group.

Collection of serum samples

For patients, peripheral venous blood (5 mL) was collected after overnight fasting before treatment, at 24 hours and on day 7 post-treatment. Samples were left at room temperature for 30-60 minutes, centrifuged at 3000 rpm for 15 minutes and the supernatant was obtained. Concurrently, urine samples (10 mL) were collected. All serum and urine specimens were aliquoted into sterile EP tubes and stored frozen at -80°C, without adding protective solutions or preservatives and without repeated freeze-thaw cycles. For rats, blood samples were collected at the end of the intervention via the abdominal aorta or cardiac puncture under ether anesthesia (3-5 mL per rat). Samples were processed as above and stored at -80°C for later measurement.

ELISA

All samples were tested by ELISA according to the manufacturer's instructions. Indicators included renal function markers (Scr, BUN), oxidative stress markers (MDA, SOD) and Nrf2 pathway-related proteins.

Histopathological examination of renal tissue

Rat kidney tissues were fixed, dehydrated in graded ethanol, cleared in xylene and embedded. Sections (4 μm) were prepared for hematoxylin-eosin (HE), periodic acid-Schiff (PAS), periodic acid-silver methenamine (PASM) and Masson staining. Two experienced associate chief physicians from the pathology department used a double-blind method to observe morphological changes in renal tissue under a light microscope and score them, ensuring the objectivity and reproducibility of the observations.

Assessment of renal tubular injury

Urine samples from each group were tested using ELISA kits to measure β2-microglobulin (β2-MG), kidney injury molecule-1 (KIM-1), neutrophil gelatinase-associated lipocalin (NGAL) and liver-type fatty acid-binding protein (L-FABP).

Detection of Nrf2-pathway-related mRNA expression in renal tissue

Total RNA was extracted from renal cortex tissue using TRIzol. One microgram of RNA was reverse-transcribed into cDNA using the PrimeScript™ RT reagent Kit with gDNA Eraser. The reaction system consisted of template RNA, 5× gDNA Eraser Buffer, gDNA Eraser to remove genomic DNA, PrimeScript RT Enzyme Mix I, RT Primer Mix and RNase-free double-distilled dH2O. Reaction conditions included incubation at 42°C for 2 min, at 37°C for 15 min and then at 85°C for 5 seconds. The synthesized cDNA was stored at -20°C.

RT-qPCR

PCR was performed in a 20 μL system containing 8 μL cDNA, 10 μL SYBR Green Master Mix and 2 μL primers (for Nrf2, HO-1, NQO1 and GAPDH as internal reference). Reaction conditions: Initial denaturation at 95 °C for 10 min; 40 cycles of annealing/extension at 60°C for 1 min. Relative expression of Nrf2, HO-1 and NQO1 mRNA was calculated using the $2^{-}\Delta\Delta Ct$ method. Primer sequences are listed in Table 1.

Western blot analysis

Renal tissues were lysed and protein concentrations were determined by BCA assay. After separation and transfer, PVDF membranes were incubated overnight with primary antibodies: Nrf2 (ab62352, 1:1000), HO-1 (ab305290, 1:1000) and NQO1 (ab80588, 1:1000) and for 1 h with secondary antibodies (1:1000). GAPDH served as the loading control. Protein bands were visualized and analyzed with software.

Table 1: Primer sequences.

Primer	Sequence
Nrf2	Forward 5'-AGTCGCTTGCCCTGGATATC-3'
	Reverse 5'-GAACAGCGGTAGTATCAGCCA-3'
HO-1	Forward 5'-GCTAAGACCGCCTTCCTGCT-3'
	Reverse 5'-ACGAAGTGACGCCATCTGTGA-3'
NQO1	Forward 5'-TATCACCACTGGGGGTAGCG-3'
	Reverse 5'-GGAGTGTGGCCAATGCTGTAA-3'
GAPDH	Forward 5'-CCTCGTCCCGTAGACAAAATG-3'
	Reverse 5'-TGAGGTCAATGAAGGGGTCGT-3'

Observation indicators

Clinical patient observation indicators: Peripheral blood and urine samples were collected from patients at three time points: before treatment, 24 hours after treatment and on the 7th day after treatment, to detect the following indicators: Renal function indicators: serum creatinine, blood urea nitrogen levels; Oxidative stress indicators: serum superoxide dismutase activity, malondialdehyde levels; Nrf2 pathway molecules: mRNA and protein expression levels of Nrf2, HO-1, NQO1 in peripheral blood mononuclear cells.

Animal experiment observation indicators: Rat blood, urine and kidney tissue samples were collected at the experimental endpoint (7th day after modeling) to detect the following indicators: Renal function indicators: serum Scr, BUN levels; Renal tubular injury markers: urinary β2-microglobulin, kidney injury molecule-1, neutrophil gelatinase-associated lipocalin, liver-type fatty acid-binding protein levels; Renal histopathology: Immediately after sacrificing the rats at the experimental endpoint, kidney tissues were taken for HE, PAS, PASM and Masson staining. Tubular injury, basement membrane integrity and interstitial fibrosis were observed under a light microscope. Nrf2 pathway molecules: mRNA and protein expression levels of Nrf2, HO-1 and NQO1 in renal tissue homogenates.

Statistical analysis

SPSS 26.0 software was used for data analysis. All measurement data were first tested for normality using the Shapiro-Wilk test and for homogeneity of variance using Levene's test. Measurement data conforming to a normal distribution were expressed as mean ± standard deviation. For clinical patient data, comparisons among the three time points (before treatment, 24 h after treatment and day 7) within each group were performed using a repeated-measures ANOVA. When the main effect of time was significant, further pairwise comparisons were conducted using the Bonferroni method. Inter-group comparisons between the observation and control groups at the same time point were performed using a two-sample t-test (Welch's correction was used when variances were unequal). In animal experiments, comparisons of renal function indicators, renal tubular injury markers and Nrf2 pathway molecule expression among the three groups (control, model, treatment) were performed using one-way ANOVA. Pairwise post-hoc comparisons between groups were conducted using Tukey HSD test (when variances were homogeneous) or Games-Howell test (when variances were heterogeneous). Inter-group differences and 95% confidence intervals between the treatment group and the model group were calculated using the two independent samples t-test. All tests were two-sided and $P < 0.05$ was considered statistically significant.

RESULTS

Baseline Characteristics of Patient

A total of 67 patients were enrolled, including 39 cases in the control group (hemoperfusion alone) and 28 cases in the observation group (hemoperfusion combined with naloxone). Baseline data were compared between the two groups. The results showed no statistically significant differences between the two groups in age, sex and etiological composition ($P>0.05$). However, statistically significant differences were observed in APACHE II score and the proportion of patients with hypertension ($P<0.05$) (Table 2), suggesting selection bias between the two groups that required adjustment in subsequent analyses.

Independent effect of combined therapy on renal function and oxidative stress markers

After controlling for confounding factors including APACHE II score, hypertension history and pre-treatment Scr level, multivariate linear regression analysis showed that combined naloxone therapy was an independent influencing factor for Scr improvement on day 7 post-treatment (adjusted $\beta = -7.94$, 95% CI: -11.86 ~ -4.02, $P < 0.001$). Repeated-measures ANOVA showed significant interactions between the time factor and the group factor on Scr, BUN, SOD and MDA levels ($P < 0.05$ for all). In both groups, the above indicators improved significantly at each time point compared with baseline (within-group comparisons, $P < 0.05$). After adjusting for confounding factors, the observation group showed significantly greater improvements in all indicators than the control group at 24 h and day 7 post-treatment ($P < 0.05$) and the improvement effect at day 7 was superior to that at 24 h (Table 3).

Table 2: Baseline characteristics of patients in the two groups.

Characteristic	Control group (n=39)	Observation group (n=28)	t/χ^2	P value
Age (years)	44.38 ± 4.53	44.86 ± 3.43	-0.476	0.636
Sex (male/female)	22/17	15/13	0.081	0.776
APACHE II score	18.64 ± 3.86	21.43 ± 4.62	-2.654	0.01
Hypertension [n (%)]	8 (20.51)	12 (42.86)	3.994	0.046
Diabetes mellitus [n (%)]	5 (12.82)	4 (14.29)	0.03	0.863
Pre-treatment Scr (μmol/L)	386.47 ± 52.75	419.38 ± 45.96	-2.667	0.015
Pre-treatment BUN (mmol/L)	19.85 ± 3.42	18.47 ± 4.16	1.489	0.141
Etiology [n (%)]	-	-	0.62	0.961
Organophosphorus poisoning	8 (20.51)	6 (21.43)	-	-
Fish gallbladder poisoning	9 (23.08)	6 (21.43)	-	-
Mushroom poisoning	9 (23.08)	6 (21.43)	-	-
Aminoglycoside poisoning	7 (17.95)	5 (17.86)	-	-
Others	6 (15.38)	5 (17.85)	-	-

Table 3: Comparison of renal function and oxidative stress indicators between the two groups at different time points.

Group	n	Time	BUN (mmol/L)	Scr (μmol/L)	MDA (μmol/L)	SOD (IU/L)
Control	39	Before treatment	19.85 ± 3.42	386.47 ± 52.75	7.28 ± 1.04	89.66 ± 8.93
		24 h post-treatment	14.36 ± 2.87*	283.49 ± 25.52*	6.68 ± 1.04*	94.74 ± 9.16*
		7th day post-treatment	10.28 ± 2.13*#	241.27 ± 20.37*#	5.99 ± 0.83*#	101.71 ± 10.52*#
Observation	28	Before treatment	18.47 ± 4.16	419.38 ± 45.96	7.15 ± 1.10	90.11 ± 9.34
		24 h post-treatment	11.82 ± 2.54*&	231.54 ± 23.48*&	5.07 ± 0.82*&	101.71 ± 10.52*&
		7th day post-treatment	8.35 ± 1.86*&#	159.66±15.22*&#	4.38 ± 0.61*&#	114.32±11.48*&#
Ftime			164.28***	438.62***	187.43***	318.56***
Fgroup			6.82**	12.47***	9.85***	15.24***
Finteraction			5.47**	8.93***	7.21***	10.37***

*Note: Data are presented as adjusted mean ± standard deviation. *P < 0.05 vs. before treatment within the same group; #P < 0.05 vs. 24 h post-treatment within the same group; †P < 0.05 vs. control group at the same time point. ***P < 0.001, *P < 0.01. F values are from repeated-measures ANOVA with adjustment for confounding factors (APACHE II score, hypertension and pre-treatment Scr).

Table 4: Comparison of Nrf2 pathway molecule expression between the two groups at different time points.

Group	n	Time	Nrf2		HO-1		NQO1	
			mRNA (fold change)	Protein (relative expression)	mRNA (fold change)	Protein (relative expression)	mRNA (fold change)	Protein (relative expression)
Control	39	Before treatment	0.27 ± 0.09	0.30 ± 0.06	0.40 ± 0.05	0.44 ± 0.08	0.50 ± 0.05	0.54 ± 0.10
		24 h post-treatment	0.36 ± 0.10*	0.41 ± 0.07*	0.52 ± 0.06*	0.55 ± 0.07*	0.57 ± 0.08*	0.63 ± 0.10*
		7th day post-treatment	0.45 ± 0.11*#	0.48 ± 0.08*#	0.60 ± 0.07*#	0.62 ± 0.08*#	0.63 ± 0.09*#	0.68 ± 0.11*#
Observation	28	Before treatment	0.31 ± 0.10	0.34 ± 0.07	0.43 ± 0.08	0.46 ± 0.07	0.57 ± 0.09	0.61 ± 0.08
		24 h post-treatment	0.46 ± 0.11*†	0.51 ± 0.08*†	0.62 ± 0.06*†	0.64 ± 0.05*†	0.66 ± 0.08*†	0.72 ± 0.06*†
		7th day post-treatment	0.56 ± 0.12*†#	0.59 ± 0.08*†#	0.71 ± 0.07*†#	0.73 ± 0.06*†#	0.74 ± 0.08*†#	0.80 ± 0.07*†#
Ftime			135.68***	185.42***	312.47***	425.73***	98.47***	146.82***
Fgroup			18.56***	22.47***	28.53***	35.81***	15.69***	20.43***
Finteraction			12.37***	16.85***	19.64***	24.56***	10.82***	14.76***

Independent effect of combined therapy on Nrf2 pathway molecule expression

After adjusting for confounding factors, multivariate linear regression analysis showed that combined naloxone therapy was an independent factor influencing the increase in Nrf2 expression level on day 7 post-treatment (adjusted β = 0.43, 95% CI: 0.27-0.59, P < 0.001). Repeated-measures ANOVA showed significant interactions between the time and group factors for the expression levels of Nrf2, HO-1 and NQO1 (P < 0.05 for all). In both groups, the above indicators increased significantly at each time point compared with baseline (within-group comparisons, P < 0.05). After adjusting for confounding factors, the observation group showed significantly higher expression levels of all indicators than the control group at each post-treatment time point (P < 0.05), peaking on day 7 (Table 4).

Table 5: Comparison of renal function and tubular injury markers among the three groups of rats ($\bar{x} \pm s$).

Group	n	SCr (μmol/L)	BUN (mmol/L)	β_2-MG (mg·L^{-1})	KIM-1 (ng·L^{-1})	NGAL (μg·L^{-1})	L-FABP (μg·L^{-1})
Control	10	27.51±7.31	12.73±3.38	2.02±0.37	165.32±28.30	129.11±44.45	22.34±5.18
Model	10	47.10±7.23*	17.78±1.13*	7.21±0.67*	646.59±18.35*	581.09±32.93*	58.18±9.26*
Treatment	10	34.35±6.16*#	14.30±2.83*#	3.11±0.71*#	301.48±53.74*#	188.33±125.06#	41.68±11.05*#
F	-	20.644	9.676	61.842	137.592	29.041	12.341
P	-	<0.001	0.001	<0.001	<0.001	0.001	0.008

Note: Data are presented as mean ± standard deviation. Rats in the control group received an intraperitoneal injection of an equal volume of normal saline; rats in the model group received a single intraperitoneal injection of cisplatin (6 mg/kg) to establish a toxic ARF model; rats in the treatment group received an intraperitoneal injection of naloxone hydrochloride (1.0 mg/kg) at 24 h post-modeling and underwent simulated hemoperfusion at 6 h post-modeling (n=10/group). *P < 0.05 compared with the control group; #*P* < 0.05 compared with the model group. Comparisons among the three groups were performed using one-way ANOVA, with homogeneity of variance confirmed by Levene's test; pairwise post-hoc comparisons between groups were performed using Tukey HSD test.

Naloxone hydrochloride combined with hemoperfusion reduces Scr and BUN levels in rats

Compared with the control group, the Scr and BUN levels in the model group were significantly increased ($P < 0.05$), indicating the successful establishment of the cisplatin-induced ARF model. Compared with the model group, the Scr and BUN levels in the treatment group were significantly reduced (Scr: 34.35 ± 6.16 vs. 47.10 ± 7.23 μmol/L, $P < 0.001$; BUN: 14.30 ± 2.83 vs. 17.78 ± 1.13 mmol/L, $P = 0.001$), but remained higher than those in the control group ($P < 0.05$). Regarding early renal tubular injury markers, the levels of β2-MG, KIM-1, NGAL and L-FABP in the model group were significantly higher than those in the control group ($P < 0.001$). After combined treatment, all four injury marker levels in the treatment group decreased significantly (P < 0.05 vs. the model group), among which NGAL levels decreased to levels not significantly different from those in the control group ($P > 0.05$; Table 5).

Naloxone hydrochloride combined with hemoperfusion significantly improved renal tissue injury in rats

Renal histopathological examination further confirmed the renoprotective effect of the combined treatment. HE staining showed that the renal tubules of rats in the control group had a clear structure, neatly arranged epithelial cells and no obvious damage. Rats in the model group showed extensive vacuolar degeneration, necrosis, shedding of renal tubular epithelial cells, lumen dilation, cast formation and severe destruction of renal tubular structure. The above pathological changes were significantly alleviated in the treatment group, with only a small amount of focal swelling of renal tubular epithelial cells and the renal tubular structure was relatively intact. PAS staining showed that the basement membrane of renal tubules in the model group was locally wrinkled, the structure was unclear and the brush border was shed; in the treatment group, the basement membrane structure was relatively intact and brush border damage was significantly reduced. Masson staining revealed extensive collagen fiber deposition in the renal interstitium of the model group, which was significantly reduced in the treatment group (Fig. 1).

Effects of naloxone hydrochloride combined with hemoperfusion on Nrf2-pathway-related mRNA expression in rats

Compared with the control group, the mRNA expression levels of Nrf2, HO-1 and NQO1 in the renal tissue of rats in the model group were significantly reduced ($P < 0.001$), with decreases of 57.9%, 62.5% and 55.6%, respectively. Compared with the model group, the expression levels of the above genes in the treatment group were significantly increased ($P < 0.001$), among which Nrf2 mRNA levels recovered to levels not significantly different from those of the control group ($P > 0.05$; Table 6).

Effects of naloxone hydrochloride combined with hemoperfusion on Nrf2-pathway-related protein expression in rats

Western blot analysis results were consistent with the mRNA expression trends. The protein expression levels of Nrf2, HO-1 and NQO1 in the renal tissue of rats in the model group were significantly lower than those in the control group ($P < 0.001$). The protein expression levels of the above indicators in the treatment group were significantly higher than those in the model group ($P < 0.001$), among which Nrf2 protein expression recovered to levels not significantly different from the control group ($P > 0.05$), while HO-1 and NQO1 protein expression, although significantly increased, remained lower than those in the control group (Fig. 2).

DISCUSSION

Toxic acute renal failure is frequently accompanied by severe oxidative stress, which leads to rapid deterioration of renal function, increases the difficulty of clinical management and results in poor prognosis (Kim *et al*., 2023).

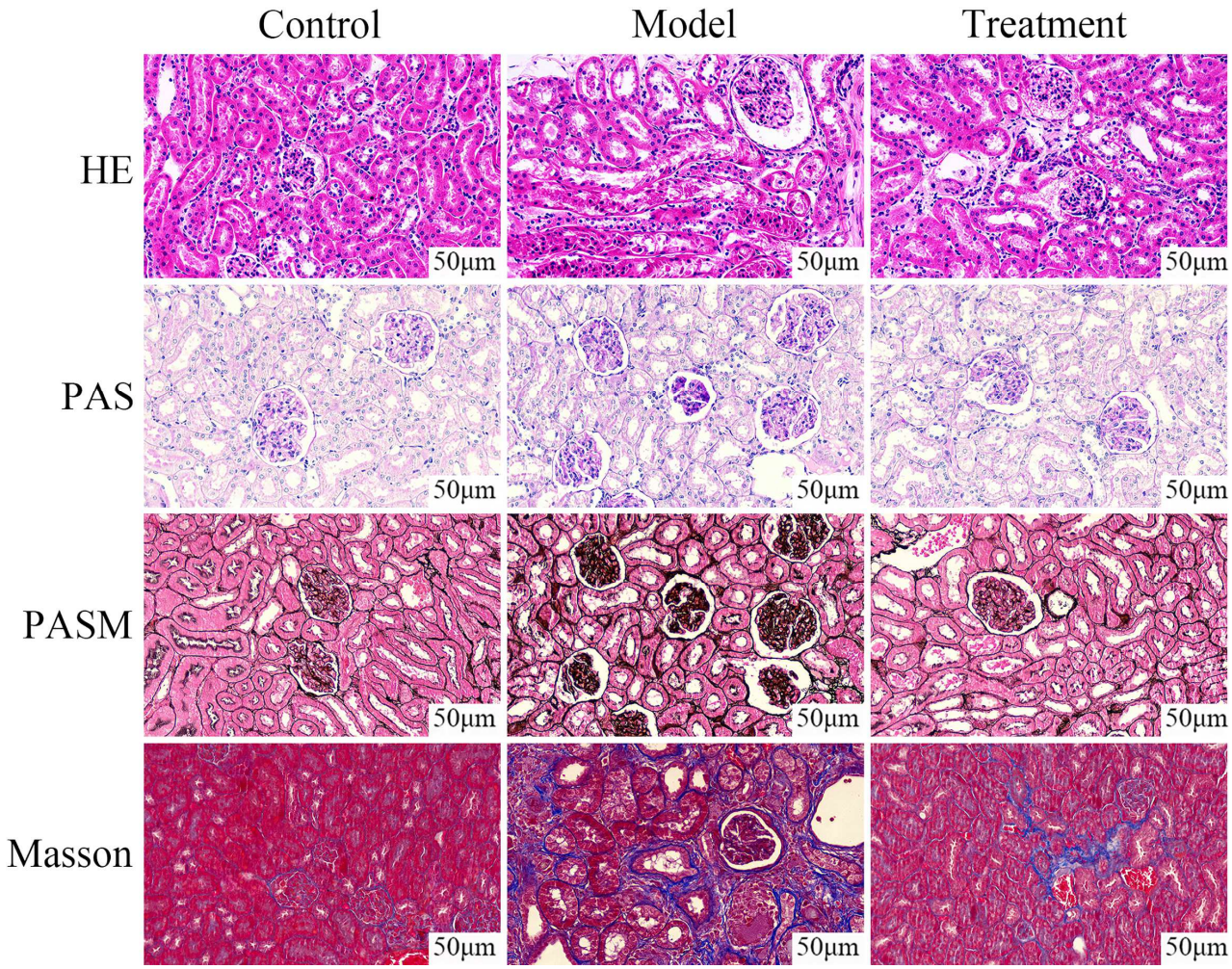

Fig. 1: Histopathological effects of naloxone hydrochloride combined with hemoperfusion on renal tissues in rats.
Note: Representative images show kidney tissue sections from rats in the control, model, and treatment groups. Scale bar = 50 μm, applies to all images. The model group exhibits typical characteristics of tubular injury and interstitial fibrosis. The treatment group shows significant pathological improvement.

Table 6: Comparison of renal tissue Nrf2-related gene mRNA expression among the three groups ($\bar{x}$±s).

Group	n	Nrf2	HO-1	NQO1
Control	10	1.52±0.10	2.51±0.09	2.43±0.09
Model	10	0.64±0.03*	0.94±0.06*	1.08±0.03*
Treatment	10	1.49±0.09#	2.14±0.18*#	1.82±0.06*#
F	-	118.247	137.477	326.452
P	-	<0.001	<0.001	<0.001

Note: Data are presented as mean ± standard deviation. Rats in the control group received an intraperitoneal injection of an equal volume of normal saline; rats in the model group received a single intraperitoneal injection of cisplatin (6 mg/kg) to establish a toxic ARF model; rats in the treatment group received an intraperitoneal injection of naloxone hydrochloride (1.0 mg/kg) at 24 h post-modeling and underwent simulated hemoperfusion at 6 h post-modeling (n=10/group). mRNA expression levels were detected by RT-qPCR, with GAPDH as an internal reference, and relative expression was calculated using the $2^{-}\Delta\Delta Ct$ method. *$P < 0.05$ compared with the control group; #$P < 0.05$ compared with the model group. Comparisons among the three groups were performed using one-way ANOVA; data conformed to normal distribution (Shapiro-Wilk test, $P > 0.05$) and homogeneity of variance (Levene's test, $P > 0.05$); pairwise post-hoc comparisons between groups were performed using Tukey HSD test. F and P values are from the overall ANOVA test.

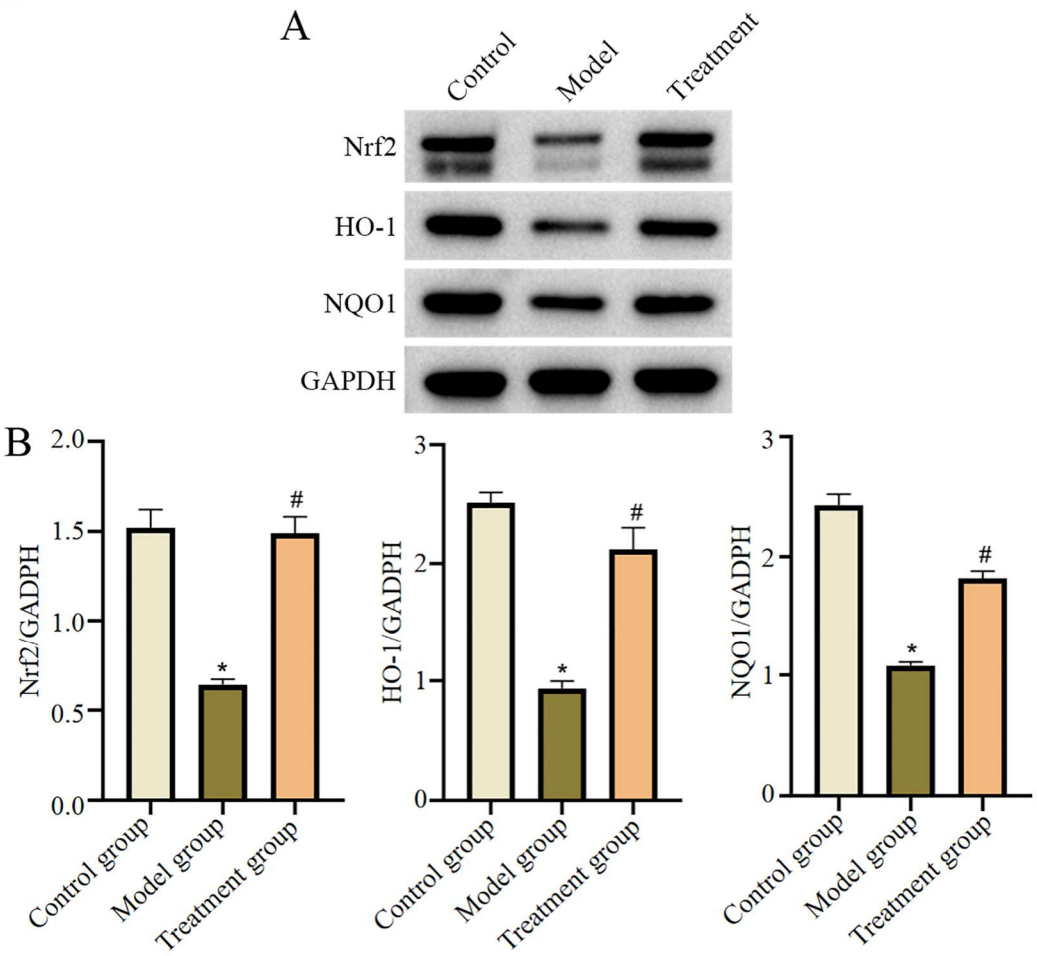

Fig. 2: Western blot detection of Nrf2, HO-1, and NQO1 protein expression in rat kidney tissues from each group.
Note: (A) Representative Western blot bands; (B) Quantitative analysis of gray values for Nrf2, HO-1 and NQO1 protein expression. Data are presented as mean ± standard deviation. *$P < 0.05$ vs. control group; #$P < 0.05$ vs. model group. Comparisons among the three groups were performed using one-way ANOVA; data conformed to normal distribution (Shapiro-Wilk test, $P > 0.05$) and homogeneity of variance (Levene's test, $P > 0.05$); pairwise post-hoc comparisons between groups were performed using Tukey HSD test. Nrf2, nuclear factor erythroid 2-related factor 2; HO-1, heme oxygenase-1; NQO1, NAD(P)H: quinone oxidoreductase 1; GAPDH, glyceraldehyde-3-phosphate dehydrogenase.

Previous studies have demonstrated that hemoperfusion effectively eliminates toxins and inflammatory mediators from the body, thereby creating favorable conditions for renal recovery (Leano *et al*., 2024). Naloxone hydrochloride, a classical opioid receptor antagonist, has been found in recent years to possess non-opioid receptor-dependent antioxidant and anti-inflammatory activities (Ibrahim *et al*., 2023). This study is the first to combine naloxone with hemoperfusion and observe significant synergistic effects. This synergy may stem from the mechanistic complementarity of the two treatment modalities: hemoperfusion rapidly clears circulating toxins, reducing the exogenous injury burden; while naloxone enhances endogenous antioxidant defense capacity at the cellular level. For instance, previous studies have demonstrated that hemoperfusion combined with hemodialysis can improve inflammatory cytokine levels in patients with end-stage renal disease (Cheng *et al*., 2022); related studies have also found that this combination therapy can correct serum calcium and phosphorus metabolism disorders in patients with chronic kidney disease and improve their renal function (Li *et al.*, 2023). Although these studies used hemodialysis rather than a drug combination, their therapeutic approach, which bases blood purification as a foundation and adds multi-target intervention as a supplement, aligns with the concept of this study. These findings collectively suggest that multi-target intervention may be an important direction for the future treatment of acute kidney injury.

The present study revealed that naloxone hydrochloride combined with hemoperfusion significantly reduced Scr and BUN levels in both patients and rats, alleviated renal histopathological damage and activated the Nrf2 signaling pathway, resulting in the upregulation of HO-1 and NQO1 expression and attenuation of oxidative stress. These

findings are consistent with the established role of the Nrf2 pathway as a crucial cellular antioxidant defense mechanism (Gao *et al*., 2026).

Our retrospective clinical data demonstrated that naloxone hydrochloride combined with hemoperfusion was independently associated with significant improvement in renal function in patients with toxic acute renal failure. After controlling for confounding factors, including APACHE II score, history of hypertension and pre-treatment Scr level, multivariate linear regression analysis revealed that combined therapy was an independent predictor of Scr reduction on day 7 post-treatment (adjusted $\beta = -8.52$, 95% CI: -12.37 to -4.67, $P < 0.001$). At 24 h post-treatment, Scr and BUN levels had already decreased significantly from baseline and further declines were observed on day 7, suggesting continued recovery of renal function. A possible explanation for these findings is that hemoperfusion rapidly removes exogenous toxins and metabolic waste products, thereby reducing the burden of direct renal injury (Butt *et al*., 2024), while naloxone hydrochloride may promote glomerular filtration by activating the Nrf2/HO-1 pathway and alleviating oxidative stress (Ibrahim *et al*., 2023). Previous studies have demonstrated that hemoperfusion effectively eliminates toxins and inflammatory mediators from the body, thereby creating favorable conditions for renal recovery (Leano *et al*., 2024; Cheng *et al*., 2022) showed that hemoperfusion combined with hemodialysis can improve inflammatory factor levels in patients with end-stage renal disease; Li *et al*. (2023) found that hemoperfusion combined with hemodialysis can correct serum calcium and phosphorus metabolism disorders and enhance renal function in patients with chronic kidney disease. Although these studies used hemodialysis rather than a drug combination, their therapeutic approach, which bases blood purification as a foundation and adds multi-target intervention as a supplement, aligns with the concept of this study. These findings collectively suggest that multi-target intervention may be an important direction for the future treatment of acute kidney injury. Although the retrospective design precludes establishing a causal relationship, the observed independent association after rigorous statistical adjustment supports the potential therapeutic benefit of this combination strategy.

Moreover, this study demonstrated a significant increase in SOD activity and reduction in MDA levels following combined therapy, with changes more pronounced by day 7. After adjusting for baseline imbalances, the observation group showed significantly greater improvements in oxidative stress markers than the control group at both 24 h and day 7 post-treatment. This suggests that naloxone hydrochloride combined with hemoperfusion is associated with improved oxidative stress status in patients with toxic acute renal failure. Lipid peroxidation resulting from excessive ROS generation is a core marker of oxidative stress, reflected by elevated malondialdehyde levels and altered superoxide dismutase activity (Alharbi and Aldubayan, 2025). Excessive ROS directly attack renal tubular epithelial cell membranes, leading to necrosis and cell shedding; thus, reducing oxidative stress is central to renal protection (Mukhi *et al*., 2023). These findings are consistent with the established role of the Nrf2 pathway as a crucial cellular antioxidant defense mechanism (Gao *et al*., 2026). The observed improvements in oxidative markers, even after adjustment for confounding variables, support the hypothesis that the combination therapy exerts antioxidant effects beyond those expected from hemoperfusion alone.

In addition, this study confirmed significant upregulation of Nrf2 and its downstream target genes, HO-1 and NQO1, within 24 h of treatment, with peak levels at day 7. Multivariate regression analysis further identified combined therapy as an independent factor associated with elevated Nrf2 expression on day 7 (adjusted $\beta = 0.47$, 95% CI: 0.31 ~ 0.63, $P < 0.001$), suggesting that the observed molecular changes cannot be fully attributed to baseline differences between groups. Mechanistic analysis suggests that under normal conditions, Nrf2 binds to Keap1 and undergoes proteasomal degradation (Chen *et al*., 2025). Naloxone hydrochloride may inhibit Keap1 ubiquitination, preventing Nrf2 degradation and stabilizing its activity (Rastinpour *et al*., 2025). Furthermore, naloxone hydrochloride may promote nuclear translocation of Nrf2, which binds to AREs and activates transcription of HO-1 and NQO1 (Asghar *et al*., 2025). HO-1 catalyzes the degradation of heme to generate bilirubin and carbon monoxide, both of which have antioxidant and anti-inflammatory properties (Stec *et al*., 2022). Along with NQO1, which detoxifies quinones and reduces free radical generation, these pathways collectively enhance cellular antioxidant defenses, alleviate lipid peroxidation, protein denaturation and DNA damage in tubular epithelial cells, thereby maintaining renal integrity (Qiu *et al*., 2023). In the animal model, the synchronous upregulation of Nrf2, HO-1 and NQO1 mRNA and protein expression indicates that the combined treatment acts at the transcriptional level rather than simply regulating protein stability. These findings are consistent with previous studies, which also demonstrated in a cisplatin-induced AKI model that Coptis root can significantly upregulate the expression of HO-1 and NQO1 by activating the Nrf2/HO-1 signaling pathway, thereby alleviating oxidative stress, mitochondrial dysfunction and renal cell apoptosis (Wu *et al*., 2023). Notably, in this study, Nrf2 mRNA and protein expression recovered to near-normal levels after treatment, whereas HO-1 and NQO1, although significantly increased, remained below normal. This difference may reflect the multilevel regulatory mechanism of the Nrf2 pathway: as a transcription factor, minimal activation of Nrf2 can initiate a cascade effect amplifying downstream gene expression. Related reports indicate that, although the gene expression levels of Nrf2 and KEAP1 did not show significant

differences across different stages of chronic kidney disease (CKD), the expression level of its downstream target gene NQO1 was significantly higher in CKD stage G3b compared with other stages, suggesting that the endogenous activation of the Nrf2 pathway primarily occurs at the functional level rather than at the transcriptional level (Timimi *et al*., 2025). However, given the retrospective nature of the clinical data, the observed Nrf2 upregulation represents an association rather than a proven mechanistic pathway; the causal relationship requires confirmation through prospective mechanistic studies.

Animal experiments further supported these observational findings. A single intraperitoneal injection of cisplatin induced marked increases in Scr and BUN in rats, confirming successful establishment of the toxic acute renal failure model (Kim *et al*., 2022). Histological observations revealed extensive tubular dilation, cast formation and vacuolar degeneration, consistent with the typical pathological hallmarks of cisplatin-induced nephrotoxicity (Alrfaei *et al*., 2023). Following combined treatment, rats in the treatment group showed significantly improved Scr and BUN levels and ameliorated renal pathology compared with the model group, indicating that naloxone hydrochloride combined with hemoperfusion can effectively reverse cisplatin-induced renal injury. After treatment, the levels of β2-MG, KIM-1, NGAL and L-FABP in rat urine significantly decreased and were negatively correlated with upregulation of the Nrf2 pathway. Previous studies in murine acute kidney injury (AKI) models have demonstrated that 4-OI can similarly reduce Ngal levels and alleviate renal tubular injury by activating the Nrf2 pathway, suggesting that the Nrf2 pathway may serve as a critical bridge linking oxidative stress to renal tubular injury (Xu *et al.*, 2023) Mechanistically, activated Nrf2 pathway reduces ROS and MDA levels by upregulating HO-1 and NQO1, thereby attenuating oxidative damage to proteins and DNA in tubular epithelial cells (Jiang *et al*.,2024). Additionally, Nrf2 activation alters the Bcl-2/Bax ratio, inhibits Caspase-3 activation and induces anti-apoptotic proteins, promoting cell survival over apoptosis and thereby further stabilizing tubular epithelial cells (Radan *et al*., 2025). These mechanisms collectively contribute to reduced tubular injury markers. Notably, the controlled experimental conditions in the animal model provide complementary causal evidence supporting the associations observed in the retrospective clinical cohort, strengthening the overall conclusion that this combination strategy confers renoprotective effects through activation of the Nrf2 pathway.

In the animal model, the synchronous upregulation of Nrf2, HO-1 and NQO1 mRNA and protein expression indicates that the combined treatment acts at the transcriptional level rather than simply regulating protein stability. These findings are consistent with previous studies, which also demonstrated in a cisplatin-induced AKI model that Coptis root can significantly upregulate the expression of HO-1 and NQO1 by activating the Nrf2/HO-1 signaling pathway, thereby alleviating oxidative stress, mitochondrial dysfunction and renal cell apoptosis(Wu *et al*., 2023). Notably, in this study, Nrf2 mRNA and protein expression recovered to near-normal levels after treatment, whereas HO-1 and NQO1, although significantly increased, remained below normal. This difference may reflect the multilevel regulatory mechanism of the Nrf2 pathway: as a transcription factor, minimal activation of Nrf2 can initiate a cascade effect amplifying downstream gene expression. Related reports indicate that, although the gene expression levels of Nrf2 and KEAP1 did not show significant differences across different stages of chronic kidney disease (CKD), the expression level of its downstream target gene NQO1 was significantly higher in CKD stage G3b compared with other stages, suggesting that the endogenous activation of the Nrf2 pathway primarily occurs at the functional level rather than at the transcriptional level (Timimi *et al*., 2025). After treatment, the levels of β2-MG, KIM-1, NGAL and L-FABP in rat urine significantly decreased and were negatively correlated with upregulation of the Nrf2 pathway. Previous studies in murine models of acute kidney injury (AKI) have demonstrated that 4-OI can similarly reduce NGAL levels and alleviate renal tubular injury by activating the Nrf2 pathway, suggesting that the Nrf2 pathway may serve as a critical bridge linking oxidative stress to renal tubular injury (Xu *et al*., 2023). Mechanistically, the activated Nrf2 pathway reduces ROS and MDA levels by upregulating HO-1 and NQO1, thereby attenuating oxidative damage to proteins and DNA in tubular epithelial cells (Jiang *et al*., 2024). Additionally, Nrf2 activation alters the Bcl-2/Bax ratio, inhibits Caspase-3 activation and induces anti-apoptotic proteins, promoting cell survival over apoptosis and thereby further stabilizing tubular epithelial cells (Radan *et al*., 2025). These mechanisms collectively contribute to reduced tubular injury markers.

This study is a small-sample, single-center, short-term study and only the cisplatin model was used. Future multi-center, long-term follow-up studies are needed to validate generalizability in other poisoning models. Furthermore, although the study confirmed Nrf2 pathway activation, a causal relationship between Nrf2 pathway activation and the renoprotective effect cannot be established and the precise molecular mechanism by which naloxone regulates the Nrf2 pathway remains unclear. Future research should use Nrf2-specific inhibitors in animal models to verify whether the renoprotective effect of the combined treatment disappears after blocking the Nrf2 pathway, construct renal tubular epithelial cell-specific Nrf2 knockout mice to determine whether the combined treatment fails after gene knockout and conduct additional experiments to further validate the findings.

CONCLUSION

In conclusion, naloxone hydrochloride combined with hemoperfusion significantly improves renal function in patients with toxic acute renal failure, alleviates histopathological injury and activates the Nrf2/HO-1/NQO1 signaling pathway to enhance antioxidative capacity. This combined strategy offers new insights for clinical management of toxic acute renal failure and provides a theoretical basis for the development of novel Nrf2-targeted renoprotective agents. However, the results of this study are primarily based on correlation analyses; the definitive causal relationship requires further validation using Nrf2 inhibitors or gene knockout models.

Acknowledgments
We gratefully acknowledge The First Affiliated Hospital of Qiqihar Medical University for providing the necessary equipment for this study.

Author's contributions
Yin Zhu: Conceptualization, methodology, investigation, formal analysis, writing–original draft, writing–review and editing; Huichun Sun: Investigation, data curation and validation; Qiuyang Wang: Investigation, formal analysis and visualization; Yong Sheng: Resources, investigation and validation; Yanli Li: Investigation and data curation; Qiang Zhang: Conceptualization, methodology, supervision, project administration, funding acquisition, writing–review and editing. All authors read and approved the final manuscript.

Funding
There was no funding.

Data availability statement
The datasets generated and/or analysed during the current study are available from the corresponding author on reasonable request.

Ethical approval
This study was approved by the Ethics Committee of The First Affiliated Hospital of Qiqihar Medical University (Approval No.: 2025-004-001). This study was performed in adherence with the STROBE and ARRIVE guidelines. See supplementary file for the STROBE and ARRIVE checklist.

Conflict of interest
The authors declare no conflict of interest.

Supplementary data
https://pjps.pk/uploads/2026/08/SUP1787915474.pdf

REFERENCES

Alam MM, Kishino A, Sung E, Sekine H, Abe T, Murakami S, Akaike T and Motohashi H (2023). Contribution of NRF2 to sulfur metabolism and mitochondrial activity. *Redox Biol.*, **60**: 102624.

Abdul Rahman H, Noraidi AA, Hj Khalid AN, Mohamad-Adam AZ, Zahari NH and Tuming NE (2025). Practical guide to calculate sample size for chi-square test in biomedical research. *BMC Med Res Methodol.*, **25**(1): 144.

Alharbi MS and Aldubayan MA (2025). Ameliorative effect of empagliflozin and linagliptin on cisplatin-induced nephrotoxicity and cardiotoxicity by reducing oxidative stress. *Drug Des Devel Ther.*, **19**: 11483–11497.

Asghar MA, Wan B, Li L, Zhang J, Tang S, Han H, Yang Y, Chu L, Zhang Q, Zhang X and Zhao Q (2025). Micronutrient antioxidant supplementation alleviates valproic acid-induced oxidative stress and male infertility via the NRF2/HO-1 pathway. *Redox Biol.*, **85**: 103685.

Alrfaei BM, Almutairi AO, Aljohani AA, Alammar H, Asiri A, Bokhari Y, Aljaser FS, Abudawood M and Halwani M (2023). Electrolytes play a role in detecting cisplatin-induced kidney complications and may even prevent them-retrospective analysis. *Medicina (Kaunas).*, **59**(5): 890.

Butt B, Mushtaq A, Hameed FA, Abbasi MSR, Tariq M, Akbar A, Jadoon SK, Tasneem S, Ahmad M, Zeb A and Alvi S (2024). Blood purification therapy in chronic renal failure and its impact on renal index, serological index and inflammatory factors. *Ann Med Surg (Lond).*, **86**(7): 3856–3864.

Cheng W, Luo Y, Wang H, Qin X, Liu X, Fu Y and Ronco C (2022). Survival outcomes of hemoperfusion and hemodialysis versus hemodialysis in patients with end-stage renal disease: A systematic review and meta-analysis. *Blood Purif.*, **51**(3): 213–225.

Chen J, Feng D, Zhu R, Li H and Chen L (2025). Advances in KEAP1-based PROTACs as emerging therapeutic modalities: Structural basis and progress. *Redox Biol.*, **85**: 103781.

Gao Y, Tang X, Yao J, Sun T, Chen Y, Cheng C, Yang J, Wang B, Liu A, Yang L and Zhao M (2026). Targeting the bile acid receptor TGR5 with gentiopicroside to activate Nrf2 antioxidant signaling and mitigate Parkinson's disease in an MPTP mouse model. *J Adv Res.*, **80**: 977-990.

Ibrahim KM, Ahmed HI, Ramadan L and Balah A (2023). A low dose of naloxone mitigates autoimmune hepatitis by regulating TLR4/NF-κB and Nrf2/HO-1 signaling pathways. *Inflammopharmacology.*, **31**(5): 2467–2478.

Jiang Z, Ye S, Wu Y, Zhou C, Cao F and Tan N (2024). Cyclopeptide RA-V from Rubia yunnanensis restores activity of Adagrasib against colorectal cancer by reducing the expression of Nrf2. *Pharmacol Res.*, **206**: 107252.

Kurzhagen JT, Noel S, Lee K, Sadasivam M, Gharaie S, Ankireddy A, Lee SA, Newman-Rivera A, Gong J, Arend LJ, Hamad ARA, Reddy SP and Rabb H (2023). T Cell Nrf2/Keap1 gene editing using CRISPR/Cas9 and experimental kidney ischemia-reperfusion injury. *Antioxid Redox Signal*., **38**(13-15): 959-973.

Kim DE, Byeon HE, Kim DH, Kim SG and Yim H (2023). Plk2-mediated phosphorylation and translocalization of Nrf2 activates anti-inflammation through p53/Plk2/p21cip1 signaling in acute kidney injury. *Cell Biol Toxicol.*, **39**(4): 1509–1529.

Kim SE, Shin HY, Lee EY, Yoo YJ, Kim RH, Cho JH, Lee TK, Ahn D, Park BY, Yoon JC, Hong S, Kim IS, Tae HJ and Won MH (2022). Effect of therapeutic hypothermia against renal injury in a rat model of asphyxial cardiac arrest: A focus on the survival rate, pathophysiology and antioxidant enzymes. *Mol Med Rep.*, **25**(1): 19.

Leano DR, Danguilan R, Arakama MH, Apelin V, Alamillo PP and Chua E (2024). Efficacy of adjunct hemoperfusion compared to standard medical therapy on 28-day mortality in leptospirosis patients with renal failure and shock: A single-center randomized controlled trial. *Trop Med Infect Dis.*, **9**(9): 206.

Li W, Wang J, Wang Y, Guan R, Zhao F and Zhang R (2023). Additional hemoperfusion for patients receiving maintenance hemodialysis: A retrospective analysis. *Am J Transl Res.*, **15**(6): 4045–4054.

Lin DW, Hsu YC, Chang CC, Hsieh CC and Lin CL (2023). Insights into the molecular mechanisms of NRF2 in kidney injury and diseases. *Int J Mol Sci.*, **24**(7): 6053.

Mukhi D, Li L, Liu H, Doke T, Kolligundla LP, Ha E, Kloetzer K, Abedini A, Mukherjee S, Wu J, Dhillon P, Hu H, Guan D, Funai K, Uehara K, Titchenell PM, Baur JA, Wellen KE and Susztak K (2023). ACSS2 gene variants determine kidney disease risk by controlling de novo lipogenesis in kidney tubules. *J Clin Invest*., **134**(4): e172963.

National Research Council (US) Committee for the update of the guide for the care and use of laboratory animals (2011). Guide for the care and use of laboratory animals. *Publication*., **327**(3): 963-965.

Qiu D, Song S, Chen N, Bian Y, Yuan C, Zhang W, Duan H and Shi Y (2023). NQO1 alleviates renal fibrosis by inhibiting the TLR4/NF-κB and TGF-β/Smad signaling pathways in diabetic nephropathy. *Cell Signal.*, **108**: 110712.

Rastinpour Z, Fakhri S, Abbaszadeh F, Ranjbari M, Kiani A, Namiq Amin M and Echeverria J (2025). Neuroprotective effects of astaxanthin in a scopolamine-induced rat model of Alzheimer's disease through antioxidant/anti-inflammatory pathways and opioid/benzodiazepine receptors: Attenuation of Nrf2, NF-κB and interconnected pathways. *Front Pharmacol.*, **16**: 1589751.

Radan M, Atefipour N, Abedizadeh P, Dayer D and Hoseinynejad K (2025). Tannic acid inhibits diquat induced human renal HK-2 cells apoptosis through BAX/Bcl2/caspase/cleaved caspase-3 signaling pathway. *Biomed Eng Online*., **24**(1): 148.

Sun YY, Zhu HJ, Zhao RY, Zhou SY, Wang MQ, Yang Y and Guo ZN (2023). Remote ischemic conditioning attenuates oxidative stress and inflammation via the Nrf2/HO-1 pathway in MCAO mice. *Redox Biol*., **66**: 102852.

Stec DE, Tiribelli C, Badmus OO and Hinds TD Jr (2022). Novel function for bilirubin as a metabolic signaling molecule: Implications for kidney diseases. *Kidney360.*, **3**(5): 945–953.

Taghavi SF, Shahsavari Z, Adjaminezhad-Fard F, Ghorbani M, Ghorbanhosseini SS, Salimi V and Tavakoli-Yaraki M (2023). Evaluating the expression pattern of the opioid receptor in pituitary neuroendocrine tumors (PitNET) and the role of morphine and naloxone in the regulation of pituitary cell line growth and apoptosis. *Biomed Pharmacother*., **157**: 114022.

Timimi A, Nagarajah S, Tepel M and Scholze A (2025). Gene expression of Nrf2 and KEAP1 in monocytes of patients with chronic kidney disease (CKD). *Int J Mol Sci.*, **26**(19): 9693.

Wang M, Liu G, Ni Z, Yang Q, Li X and Bi Z (2024). Acute kidney injury comorbidity analysis based on international classification of diseases-10 codes. *BMC Med Inform Decis Mak.*, **24**(1): 35.

Wu W, Zhang Y, Liu G, Chi Z, Zhang A, Miao S, Lin C, Xu Q and Zhang Y (2023). Potential protective effects of Huanglian Jiedu Decoction against COVID-19-associated acute kidney injury: A network-based pharmacological and molecular docking study. *Open Med (Wars)*., **18**(1): 20230746.

Xu L, Cai J, Li C, Yang M, Duan T, Zhao Q, Xi Y, Sun L, He L, Tang C and Sun L (2023). 4-Octyl itaconate attenuates LPS-induced acute kidney injury by activating Nrf2 and inhibiting STAT3 signaling. *Mol Med*., **29**(1): 58.

Yu CH, Huang LC and Su YJ (2024). Poisoning-induced acute kidney injury: A review. *Medicina (Kaunas)*., **60**(8): 1302.

Yang Q, Liu G, Guo M, Yuan D, Huang J, Zhou Z and Li Q (2025). The clinical efficacy evaluation of the KHA-200 hemoperfusion device in the treatment of end-stage renal disease patients undergoing blood purification therapy. *Kidney Dis (Basel).*, **11**(1): 270–282.

Zou LX, Wang X, Qian CH, Zheng XQ and Sun L (2026). Effect of hemoperfusion plus hemodialysis on uremic toxins and anemia in patients with maintenance hemodialysis. *Ren Fail.*, **48**(1): 2642241.